Research article

A low-cost, antimicrobial aloe-alginate hydrogel film containing Australian First Nations remedy 'lemon myrtle oil' (*Backhousia citriodora*) – Potential for incorporation into wound dressings

Dinuki M. Seneviratne [a,b,c,*], Brooke Raphael [d], Eliza J. Whiteside [a,b,c,e], Louisa C.E. Windus [a,c], Kate Kauter [a], John D.W. Dearnaley [d], Pratheep K. Annamalai [c,g], Raelene Ward [b,e,f], Pingan Song [c,d], Paulomi (Polly) Burey [c,d]

[a] *School of Health and Medical Sciences, University of Southern Queensland, Toowoomba, Queensland, Australia*
[b] *Centre for Health Research, University of Southern Queensland, Toowoomba, Queensland, Australia*
[c] *Centre for Future Materials, University of Southern Queensland, Toowoomba, Queensland, Australia*
[d] *School of Agriculture and Environmental Science, University of Southern Queensland, Toowoomba, Queensland, Australia*
[e] *Institute for Resilient Regions, University of Southern Queensland, Toowoomba, Australia*
[f] *Kunja Traditional Owner, Cunnamulla, Queensland, Australia*
[g] *School of Agriculture and Food Sustainability, The University of Queensland, Brisbane, Queensland, Australia*

ARTICLE INFO

ABSTRACT

Chronic wounds pose a global public health challenge, particularly in remote settings where access to specialised wound care and dressings can be limited and cost-prohibitive. First Nations communities in Australia are at a significantly higher risk for developing chronic wounds and this risk further increases for people living in remote regions. There is an urgent need to develop inexpensive but effective wound dressings to improve wound outcomes. Over the past decade, sodium alginate (SA)-based hydrogel polymers have emerged as a cost-effective and biocompatible component in wound dressings, and many have been successfully commercialised. In this study, we have developed and evaluated various prototypes of SA-based hydrogels with the addition of another low-cost component, aloe vera (AV) to further tailor the physicochemical properties of the hydrogel. Since the presence of microbes is a major contributor to the pathophysiology of chronic wounds, we also evaluated the antimicrobial activity of lemon myrtle oil (LMO) (*Backhousia citriodora*) incorporated into the hydrogel, a remedy used traditionally by First Nations Australians. Novel formulations of AV-SA-LMO hydrogel prototypes in the absence and presence of lemon myrtle oil (at a concentration of 5 μg/mL) were assessed for their physicochemical and antimicrobial properties and compared to a commercially available hydrogel-based dressing. The addition of lemon myrtle oil imparted viscoelastic behaviour for improved processability of AV-SA-LMO hydrogel prototypes, while increasing protein adhesion, enhancing physical properties, and demonstrating antimicrobial activity against the common wound-infecting microbes *Staphylococcus epidermidis* and *Candida albicans*. Fourier transmission infrared (FTIR) spectra confirmed the molecular structures of the hydrogel prototypes as predicted. The prototypes also demonstrated biocompatibility with the HaCaT human keratinocyte cell line. This study has provided preliminary evidence that a 25:75 aloe vera:sodium alginate hydrogel with 5 μg/mL lemon myrtle oil has comparable physicochemical characteristics to a

---

commercial hydrogel-based wound dressing and antimicrobial properties against *S. epidermidis* and *C. albicans*.

1. Introduction

Acute wounds that fail to heal within one to three months (depending on the severity of the wound) are classified as chronic wounds and are more common in older people with co-morbidities such as diabetes, hypertension, and chronic kidney disease [1]. Chronic wounds can lead to significant morbidity, marked loss of quality of life, and are a significant challenge for both patients and health professionals and a monetary burden for governments [2]. For example, in 2019, approximately 16.3 % of Medicare beneficiaries were impacted by chronic wounds, which led to a chronic wound-related cost of USD 22.5 billion [3]. In Australia, chronic wounds are a significant issue for First Nations Peoples, particularly those living in rural and remote areas [4]. The microenvironmental factors contribute to a slower healing rate of acute wounds leading to the pathogenesis of chronic wounds, which can include moisture imbalances and pathogenic microbial load (infection) [5]. Therefore, it is essential that wound dressings used in the treatment of acute wounds promote wound healing and thereby lead to the prevention of chronic wounds.

Ideal wound dressings have a biocompatible chemical composition, favourable mechanical properties, antimicrobial activity, water vapour permeability, water absorption capability, protein adsorption ability, and moisture retention [6]. In addition to these factors, the development of novel types of wound dressings should further focus on improved efficiency in promoting wound healing, cost-effectiveness, prolonged shelf-life, ease of use, and accessibility to those located in remote geographical regions [7]. Unfortunately, contemporary and novel wound dressings, including hydrogel-based dressings, are not always cost-effective since expensive materials are used to develop these products [8]. This has prompted the current study; the development and evaluation of novel hydrogel formulations that demonstrate the physical, mechanical, and biocompatibility characteristics of the hydrogels used in a commercial wound dressing but are more cost-effective to produce and incorporate Australian First Nations knowledge.

Recent research has indicated that materials of a natural origin can be a more cost-effective option for wound dressings due to their renewability and 'innate' biocompatibility [6]. Sodium alginate (SA) is a structural biopolymer derived from brown algae that is increasingly used in commercial hydrogel-based wound dressings. Sodium alginate is a linear anionic polysaccharide comprised of M-blocks (β-(1–4)-D-mannuronic acid) and G-blocks (α-L-guluronic acid) [9]. The desired structural integrity of hydrogels can be obtained by crosslinking sodium alginate using divalent calcium ions via anion-cation interactions. Aloe vera (AV) gel, consisting of polysaccharides, vitamins, enzymes, amino acids, minerals, and trace elements, is also used in wound dressings as it promotes cell proliferation and wound closure [10]. Aloe vera also offers a range of viscoelastic properties with its water-soluble oligosaccharides and saponins [11], which enable tuning the water absorption and rheological behaviour of AV-based materials.

Lemon myrtle oil (LMO) has been traditionally used as a remedy by Australian First Nations Peoples for wound care through chewing leaves directly (for oral care) or as a topical paste applied to the skin [12]. A recent Australian study reported lemon myrtle oil to have potent antimicrobial activity against Gram-positive and Gram-negative bacteria and yeasts and specific antimicrobial activity against *Staphylococcus aureus*, *Staphylococcus epidermidis*, *Escherichia coli* and *Klebsiella pneumoniae* [13]. Lemon myrtle oil has both microbiostatic and microbiocidal activities against wound-associated microbes and biofilms in the range of 10–100 μg/mL [14] and is non-toxic to human skin cells (HaCaT human keratinocyte cell line) up to 10 μg/mL [14,15]. To our knowledge, lemon myrtle oil has not been investigated as an antimicrobial component in hydrogel-based wound dressings.

This study aimed to develop and evaluate lower-cost hydrogel prototypes for potential use in wound dressings that combine the antimicrobial properties of lemon myrtle oil with the adjustable physicochemical properties of aloe vera and sodium alginate in two different ratios. To achieve this aim, the rheological, physicochemical, antimicrobial, and biocompatibility properties of AV-SA-based hydrogels at ratios of 5:95 and 25:75 formulated with and without lemon myrtle were investigated.

2. Experimental section

2.1. Materials

Sodium alginate (SA), glycerine and calcium chloride (CaCl$_2$) were purchased from Melbourne Food Ingredient Depot (Melbourne, Australia). Lemon myrtle oil (LMO) was purchased from Australian Wholesale Oils (New South Wales, Australia) and aloe vera (AV) was purchased from The Australian Superfood Company (Victoria, Australia). Phosphate-buffered saline (PBS) and bovine serum albumin (BSA) were purchased from Bio-Rad (California, USA). A commercially available HydroTac Transparent hydrogel dressing (HTT HGs) was purchased from Hartmann (New South Wales, Australia). Antimicrobial reference powders of ciprofloxacin (Sigma Aldrich, Missouri, USA) and amphotericin-B (Sigma Aldrich, Missouri, USA) were purchased from their respective manufacturers, along with Sensitest agar (Oxoid, United Kingdom), Muller-Hinton Broth (MHB) (Oxoid, United Kingdom) and Roswell Park Memorial Institute (RPMI) 1640 media (Sigma Aldrich, Missouri, USA). Other cell culture consumables included 6-well plates and pipettes (SPL Life Sciences, Korea), foetal bovine serum (FBS; Bovogen Biologicals, Victoria, Australia), Penicillin-Streptomycin (Sigma Aldrich, Victoria, Australia) and alamarBlue cell viability reagent (ThermoFisher, Oregon, USA).

2.2. Preparation of aloe-alginate-lemon myrtle oil hydrogels

Hydrogels incorporating aloe vera and sodium alginate were prepared as previously described with several modifications [16]. In brief, reverse osmosis (RO) Milli-Q water (Merck Millipore, Burlington, MA, USA) was used to prepare 1.5 % (w/v) sodium alginate and 1.0 % (w/v) aloe vera solutions. These solutions were then mixed to obtain AV:SA ratios of 5:95 and 25:75, to which glycerine was then added at 15 % (w/w, based on the mass of SA) as the plasticiser. These mixtures were then autoclaved (Atherton Gen5 series Mongoose, Australia) at 121 °C for 15 min.

After cooling the sterilised mixtures, lemon myrtle oil was filtered-sterilised (using a 0.22 μm syringe filter) (*Backhousia citriodora*) and added to the 5:95 (5:95+LMO) and 25:75 (25:75+LMO) hydrogel mixtures at a concentration of 5 μg/mL (lowest concentration demonstrated to elicit antimicrobial activity, data not included) to obtain the treatment hydrogels. Approximately 3 mL of the control (5:95C and 25:75C) and treatment (5:95+LMO and 25:75+LMO) hydrogel mixtures were then poured into sterile 6-well plates with nine replicates of each. The hydrogel films were dried at 37 °C in an oven (Memmert UF1060) for approximately 24 h. After the drying process, the hydrogels (diameter = 22 mm) were crosslinked by immersing them for 1 min in a sterile 5 % $CaCl_2$ solution and washing them in RO water before air drying at room temperature (23 ± 2 °C).

2.3. Fourier transmission infrared (FTIR) spectroscopy

The chemical compositions of the experimental and commercial hydrogels (n = 9) were evaluated by FTIR spectroscopy (Thermo Fisher Scientific Nicolet iS50 FTIR spectrometer, WI, USA). The method followed a previously established protocol [10]. The hydrogel samples were scanned at a frequency range from 4000 to 400 cm^{-1}.

2.4. HaCaT keratinocyte cell culture and biocompatibility assay

The immortalised human keratinocyte cell line (HaCaT cells; ATCC CRL-2522) was obtained from the American Type Culture Collection (ATCC). HaCaT cells were cultured in RPMI 1640 media, supplemented with 10 % FBS and 1 % Penicillin-Streptomycin. These cell cultures were maintained in a humidified atmosphere with 5 % CO_2 at 37 °C. Cells were seeded in 6-well plates at a density of 0.3×10^6 cells per well one day before introducing the hydrogels for the biocompatibility assessment.

An alamarBlue assay was conducted (as per manufacturer's guidelines) to assess the effect of the 25:75C and 25:75+LMO hydrogels on HaCaT cell numbers over 24-, 48- and 72-h periods. Respective hydrogels were added to the wells seeded with 70 % confluent HaCaT cells, while no hydrogels were added to the control wells before incubating them for their respective time periods. At each time point, cells were further incubated for approximately 3 h after resazurin was added to the wells at a 1:10 ratio. The absorbance was then measured at λ = 570 nm using a Varioskan LUX Multimode Microplate Reader (Singapore) with each sample being tested in four replicates (n = 4). Results are expressed as a percentage of cell viability compared to the control cells with no hydrogel treatment (100 %).

2.5. Swelling behaviour

The swelling behaviour of the experimental and commercial hydrogels (n = 9) was determined as a swelling percentage [17]. After drying, the hydrogels were immersed in distilled water for 24 h at room temperature (23 ± 2 °C), where the mass of the water container was weighed at 0-min, 5-min, 10-min, 15-min, 30-min, 1-h and 24-h time points. The swelling percentage (%) was calculated using the following formula:

$$Swelling\ percentage\ (\%) = \frac{W_0 - W_t}{W_{HG} - W_0} \times 100\%$$

where W_0 represents the mass of the distilled water container without the hydrogel at the 0-min time point (g), W_t represents the mass of the distilled water container with the hydrogel at the given time point (g), W_{HG} represents the mass of the distilled water container with the hydrogel at 0-min time point (g). Results are expressed as mean swelling percentage ± SEM.

2.6. Moisture content

The moisture content of the experimental and commercial hydrogels (n = 9) was evaluated by drying the swollen hydrogels at 37 °C for 24 h, where the containers with the hydrogels were weighed before and immediately after dehydrating. The moisture content (%) was calculated by:

$$Moisture\ content\ (\%) = \frac{W_f - W_i}{W_i - W_C} \times 100\%$$

where W_f represents the final mass of the container with the hydrogel after dehydration (g), W_i represents the initial mass of the container with the hydrogel before dehydration (g), W_C represents the mass of the container without the hydrogel (g). Results are expressed as mean moisture content percentage ± SEM.

2.7. Hydrogel thickness

The thickness of the experimental and commercial hydrogels (n = 9) was measured in mm using a digital Vernier calliper [6]. The results are expressed as the mean thickness (mm) ± SEM.

2.8. Rheological analysis

Rheological measurements were obtained using an Anton Paar MCR 502 Rheometer (Anton-Paar-Strasse 20, 8054, Graz, Austria) at 25 °C using parallel plates (diameter = 25 mm). A dynamic frequency sweep test was performed at $0.1–100$ rad$\cdot$s^{-1} on the experimental and commercial hydrogel discs (n = 9) at a shear strain of 0.5 %. The measured thickness of each hydrogel was set as the gap for each test, with an applied sensor force maintained at approximately 0.45 N. The storage modulus (G'; Pa), loss modulus (G''; Pa) and complex viscosity (η^*, mPa$\cdot$s) were obtained.

2.9. Water vapour transmission rate (WVTR)

The moisture permeability of experimental and commercial hydrogels (n = 9) was evaluated via the water vapour transmission rate (WVTR) as previously described [17]. Hydrogels were mounted on the mouth of a cylindrical vial (diameter = 22 mm) containing a fixed amount of distilled water and placed at 37 °C for 24 h. The WVTR was calculated for 24 h using the following formula:

$$WVTR = \frac{W_i - W_f}{A}$$

where W_i represents the initial mass of the container before the test (g), W_f represents the final mass of the container after the 24-h test (g), A represents the cross-sectional area of the film through which the vapour is transmitting (m^2). Results are expressed as mean WVTR ± SEM.

2.10. Protein adsorption assay

The protein adsorption assay was conducted according to a previously published method [17]. Experimental and commercial hydrogels (n = 9) were first placed in PBS for 24 h to achieve swelling equilibrium. The hydrogels were then placed in 300 μL of 0.5 mg/mL BSA solution in PBS and agitated in 6-well plates for 24 h at 37 °C. The hydrogels were then removed from the BSA solution and rinsed with PBS three times. The difference between the BSA concentrations in the solutions before and after the test was used to quantify the concentration of adsorbed protein by the hydrogels. The adsorbed BSA density was calculated by:

$$Adsorbed\ BSA\ density = [BSA]_S - \left(\frac{[BSA]_S}{Abs_{I\ @\ 220nm}} \times Abs_{F\ @\ 220nm} \right)$$

where $[BSA]_S$ represents the BSA concentration of the stock solution (0.5 mg/mL), $Abs_{I\ @\ 220nm}$ represents the absorbance of the BSA stock solution before the experiment at 220 nm, $Abs_{F\ @\ 220nm}$ represents the absorbance of the BSA solution after the experiment at 220 nm.

2.11. Antimicrobial activity assay

An antimicrobial activity assay was performed according to the Clinical Laboratory Standards Institute (CLSI) broth microdilution method M100-S18 [18]. Experimental and commercial hydrogels were tested for antimicrobial activity against *Staphylococcus epidermidis* (ATCC 14990) and *Candida albicans* (ATCC 18804). These microbes were subcultured onto Sensitest agar for 24 h and incubated at 37 °C, where a loop of *S. epidermidis* and *C. albicans* strains were added respectively to MHB and RPMI 1640 media to produce a 0.5 McFarland Standard solution. A 100 μL volume of MHB and RPMI without microbes were added to contamination control (CC) wells of the round-bottom 96-well plate (Sarstedt, North Rhine-Westphalia, Germany) for *S. epidermidis* and *C. albicans*, respectively. Ciprofloxacin and amphotericin-B were prepared to a concentration of 24 μg/mL in 25 % ethanol 0.9 % saline. 50 μL of 0.5 McFarland Standard solutions of MHB and RPMI with the respective microbes were added to the remaining wells. While 50 μL of sterile water and lemon myrtle oil were added to the negative control (NC) and lemon myrtle oil wells respectively, 50 μL of the 24 μg/mL ciprofloxacin and amphotericin-B solutions were added to the positive control (PC) wells to achieve a final concentration of 12 μg/mL. Experimental and commercial hydrogels were sterile hole-punctured, where they were placed into their respective test wells.

The 96-well plate was incubated for 24 h at 37 °C, where microbial growth was observed and reported as no growth, growth or full growth. Then, the MHB and RPMI media from the respective wells were streaked onto Sensitest agar plates and incubated for 48 h at 37 °C. The growth on Sensitest agar plates was observed to support the findings obtained from the 96-well broth microdilution plate.

2.12. Statistical analysis

Statistical analyses and visualisation were performed using GraphPad Prism Version 10.2.0 (392). Statistical significance was determined using the Kruskal-Wallis test and Dunn's Multiple Comparisons tests for post-hoc analysis. All the tests were conducted in

replicates of nine (n = 9) for all test variables unless otherwise stated. A p-value of ≤0.05 was considered to be statistically significant.

3. Results

3.1. FTIR spectroscopy analysis

FTIR spectra of the commercial and prepared hydrogel samples were analysed to determine the presence of various molecular vibrations of functional groups that are characteristic of sodium alginate, aloe vera and lemon myrtle oil (Fig. 1).

In Fig. 1a, the absorption band in the ranges of 3255–3263 cm^{-1}, 1592-1594 cm^{-1} and 1415-1416 cm^{-1} represented -OH stretching, asymmetric and symmetric COO- stretching of carboxylic groups, respectively, of alginate [19] and aloe vera [20]. The vibration band of 1082–1083 cm^{-1} was related to the presence of C-O-H bonds in sodium alginate [21], where C-C and C-O stretching indicated the proportion of the crystalline phase [22] and the presence of crosslinking [19]. This absorption band also indicated the C-O stretching of terpenoid groups in lemon myrtle oil [23] and the skeletal backbone of glycerine [24]. Stretching vibration bands observed at 1026-1027 cm^{-1} were specific to the presence of C-O-H bonds in alginate [21], which could be attributed to high-intensity C-C stretching due to either calcium ions strongly bonding with guluronic acid in sodium alginate or a strong hydroxyl bonding vibration [19]. The -CO group stretching vibrations from the C-O-C linkages in the glycosidic bonds in sodium alginate could further contribute to this band [25].

Most of the bands that are specific for lemon myrtle oil could not be identified in FTIR spectra when incorporated into the hydrogels (Fig. 1b). This could be due to these peaks being masked by or overlapping with the sodium alginate and aloe vera peaks [26]. Overall, it can be supported that the vibrational bands observed in the FTIR spectra concur with the incorporated constituents and the molecular structure of the hydrogel types.

3.2. HaCaT cell line biocompatibility

The effect of 25:75C and 25:75+LMO hydrogels on the numbers of HaCaT cells over 24, 48, and 72 h were expressed as a percentage HaCaT cell viability compared to the control group (no exposure to hydrogels) and this data is presented in Fig. 2. The HaCaT cell viability displays a significant increase of ~5.27 % in the 25:75+LMO group at 24 h compared to 25:75C. The cell viability continues to progressively increase to ~6.25 % and ~6.98 % in the 25:75+LMO group compared to 25:75C over the 48- and 72-h periods, respectively.

3.3. LMO incorporation led to decreased swelling and moisture, and increased thickness in hydrogel films

The influence of lemon myrtle oil incorporation on the swelling behaviour of the hydrogel films in aqueous solutions was measured by swelling (Fig. 3a), moisture content (Fig. 3b) and hydrogel thickness (Fig. 3d), where the relationship between the swelling behaviour of hydrogel films at 24 h and moisture percentage is displayed in Fig. 3c.

It was observed that the hydrogels with higher aloe vera and lower alginate (25:75C and 25:75+LMO) had a higher swelling capacity (Fig. 3a), moisture percentage (Fig. 3b) and hydrogel thickness (Fig. 3d) compared to the hydrogels with lower aloe vera and higher sodium alginate (5:95C and 5:95+LMO). The swelling behaviour of 25:75+LMO hydrogels was similar to the HTT HG (commercial dressing) (Fig. 3c). Similarly, 25:75C and 25:75+LMO hydrogels displayed similar moisture percentages (95.83 ± 1.97 % and 90.15 ± 1.59 %, respectively) to the commercial dressing (90.47 ± 0.23 %). The swelling behaviour had a strong positive
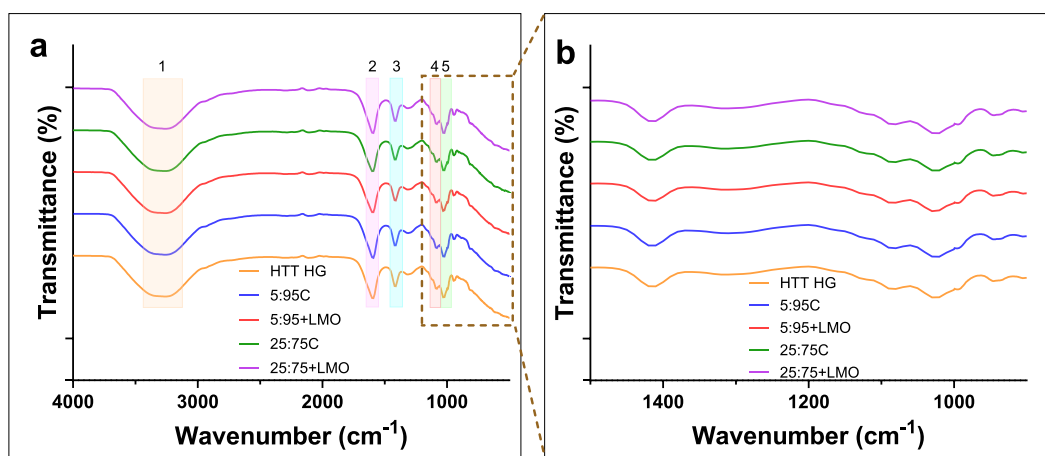

Fig. 1. Fourier transmission infrared (FTIR) spectra of the hydrogels. a) Full-scale FTIR with coloured zones represent peak numbers (cm^{-1}) represent 1) 3255–3263, 2) 1592–1594, 3) 1415–1416, 4) 1082–1083 and 5) 1026–1027. b) Magnified FTIR spectra of 900–1500 cm^{-1}.
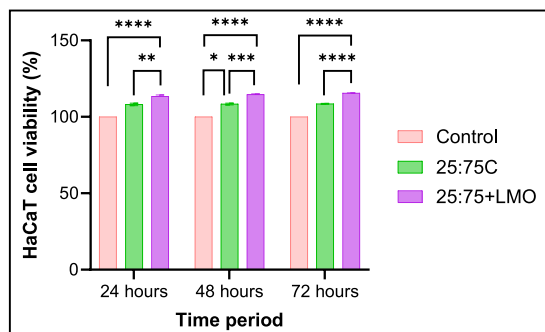
Fig. 2. Effects of 25:75C and 25:75+LMO hydrogels on HaCaT cell viability. The effects of 25:75C and 25:75+LMO hydrogels on HaCaT cell viability (%) were measured after 24-, 48- and 72-h periods via an alamarBlue assay. Data represented as mean ± SEM. Statistical significance was determined by the Kruskal-Wallis test and Dunn's multiple comparisons test. *$p \leq 0.05$, **$p \leq 0.01$, ***$p \leq 0.001$, ****$p \leq 0.0001$. Legend: ■ Control, ■ 25:75C and ■ 25:75+LMO.
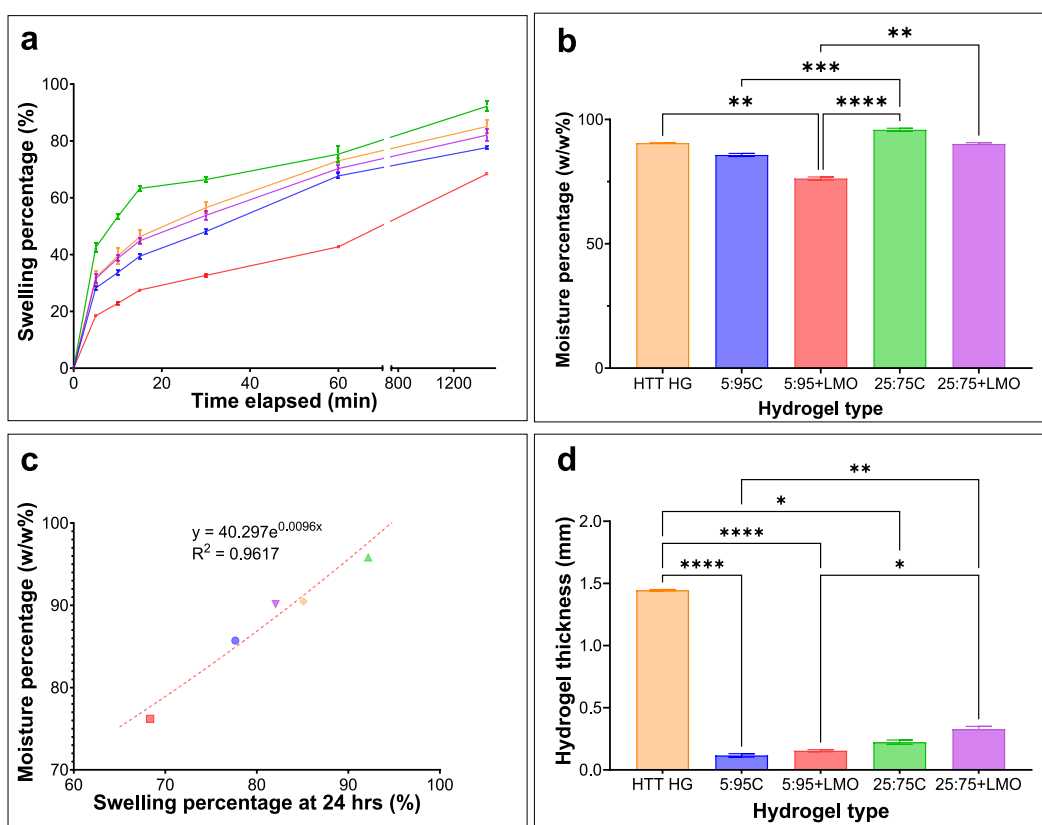

Fig. 3. Swelling and moisture percentages and hydrogel thickness of hydrogel types. a) The swelling percentage over time of the four hydrogels. Data represented as mean ± SD. b) The moisture percentage of each hydrogel after swelling. Data represented as mean ± SEM. **$p \leq 0.01$, ***$p \leq 0.001$, ****$p \leq 0.0001$ and c) the relationship between hydrogel moisture percentage and swelling percentage at 24 h. ----- represents the line of best fit for presented data sets. Legend: ◆ HTT HG (commercial dressing), ● 5:95C, ■ 5:95+LMO, ▲ 25:75C and ▼ 25:75+LMO. d) The thickness of hydrogel films as obtained for the four hydrogel types after crosslinking with CaCl$_2$. Data represented as mean ± SEM. Statistical significance was determined by the Kruskal-Wallis test and Dunn's multiple comparisons test. *$p \leq 0.05$, **$p \leq 0.01$, ****$p \leq 0.0001$.

relationship with the moisture content of the hydrogels (Fig. 3c). The average thicknesses of approximately 0.14 mm and 0.28 mm were recorded for hydrogels with high (5:95C and 5:95+LMO) and low (25:75C and 25:75+LMO) sodium alginate concentrations, respectively. The 25:75+LMO hydrogel was the thickest of the prototypes. The commercial dressing displayed a significantly greater thickness of 1.45 mm (Fig. 3d) even though its moisture percentage was not significantly different to the 25:75+LMO hydrogel

(Fig. 3b).

3.4. Rheological behaviour

The flow behaviour of the hydrogel samples was analysed through dynamic rheological measurements as displayed in Fig. 4.

The solid-like behaviour of the hydrogels is reflected by the storage modulus (G′), while the loss modulus (G″) reflects the liquid-like behaviour. The incorporation of the higher sodium alginate level led to an increase in G′ (Fig. 4a), while decreasing G″ (Fig. 4b) and η* (Fig. 4c), indicating a tendency more to solid-like behaviour. A decrease in G′ (Fig. 4a) along with an increase in both G″ (Fig. 4b) and η* (Fig. 4c) are seen as the incorporated levels of aloe vera were increased. The incorporation of lemon myrtle oil led to an increased G′ (Fig. 4a) and a decreased η* (Fig. 4c) in all hydrogel types. However, lemon myrtle oil has caused a crossover in G″ in the 5:95 hydrogel
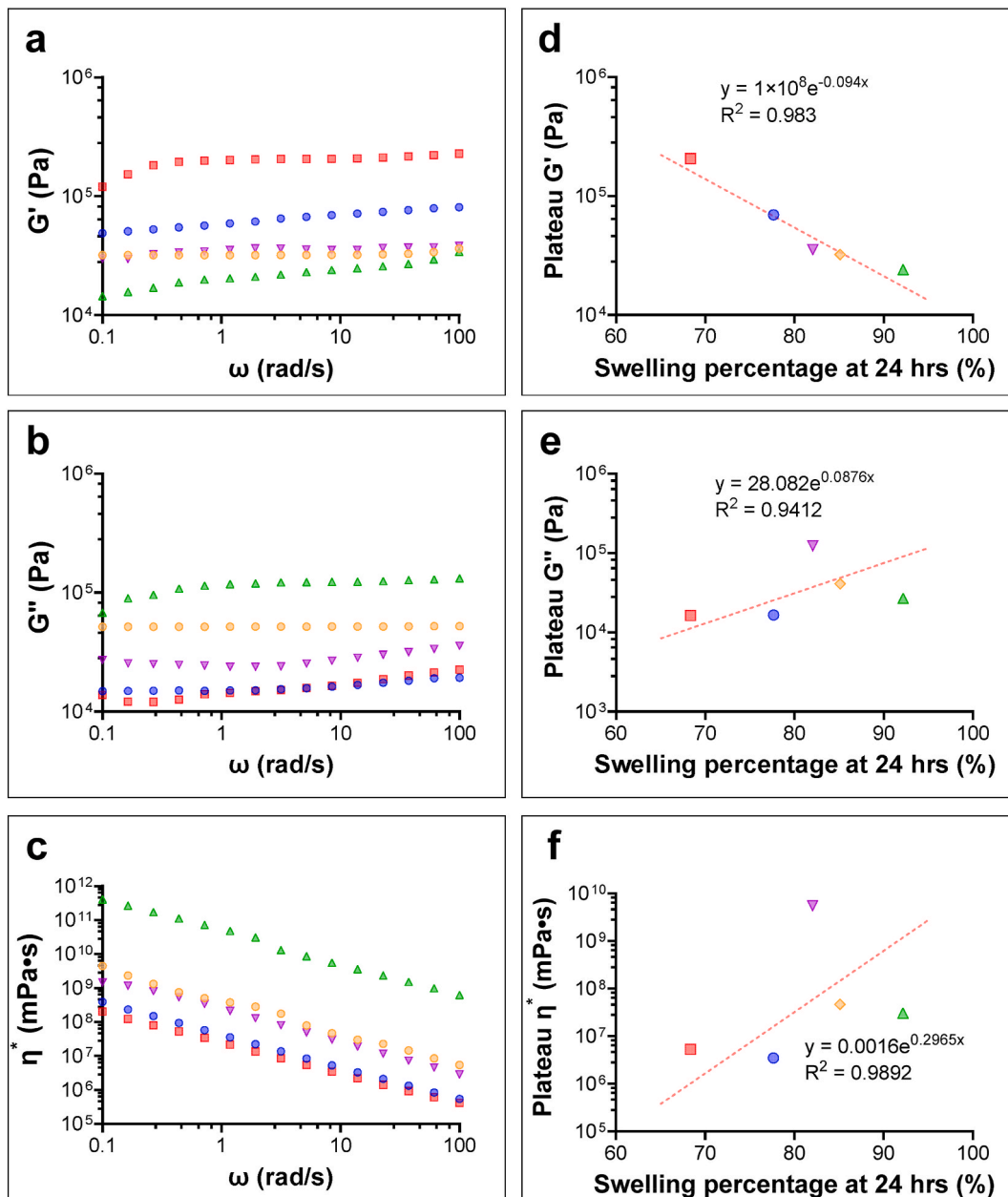

Fig. 4. Rheological behaviour of the hydrogel types. Frequency dependence of a) Storage modulus (G′), b) loss modulus (G″) and c) complex viscosity (η*) of the four hydrogel types. The relationship of d) storage modulus (G′), e) loss modulus (G″) and f) complex viscosity (η*) at 8.48 rad/s with swelling percentage at 24 h. For G′ and G″, this frequency was selected as it was in a plateau, which was then also used as a reference for η*. ----- represents the line of best fit for presented data sets. Legend: ◆ HTT HG, ● 5:95C, ■ 5:95+LMO, ▲ 25:75C and ▼ 25:75+LMO.

types (5:95C and 5:95+LMO), while G'' was decreased in 25:75+LMO compared to 25:75C (Fig. 4b). When 25:75+LMO hydrogels were compared to the 25:75C hydrogels, a decrease in G'' was displayed. Due to the strong interactions between sodium alginate molecules in 5:95C and 5:95+LMO hydrogels, an effect of lemon myrtle oil on G'' was not evident where it could be due to G' being
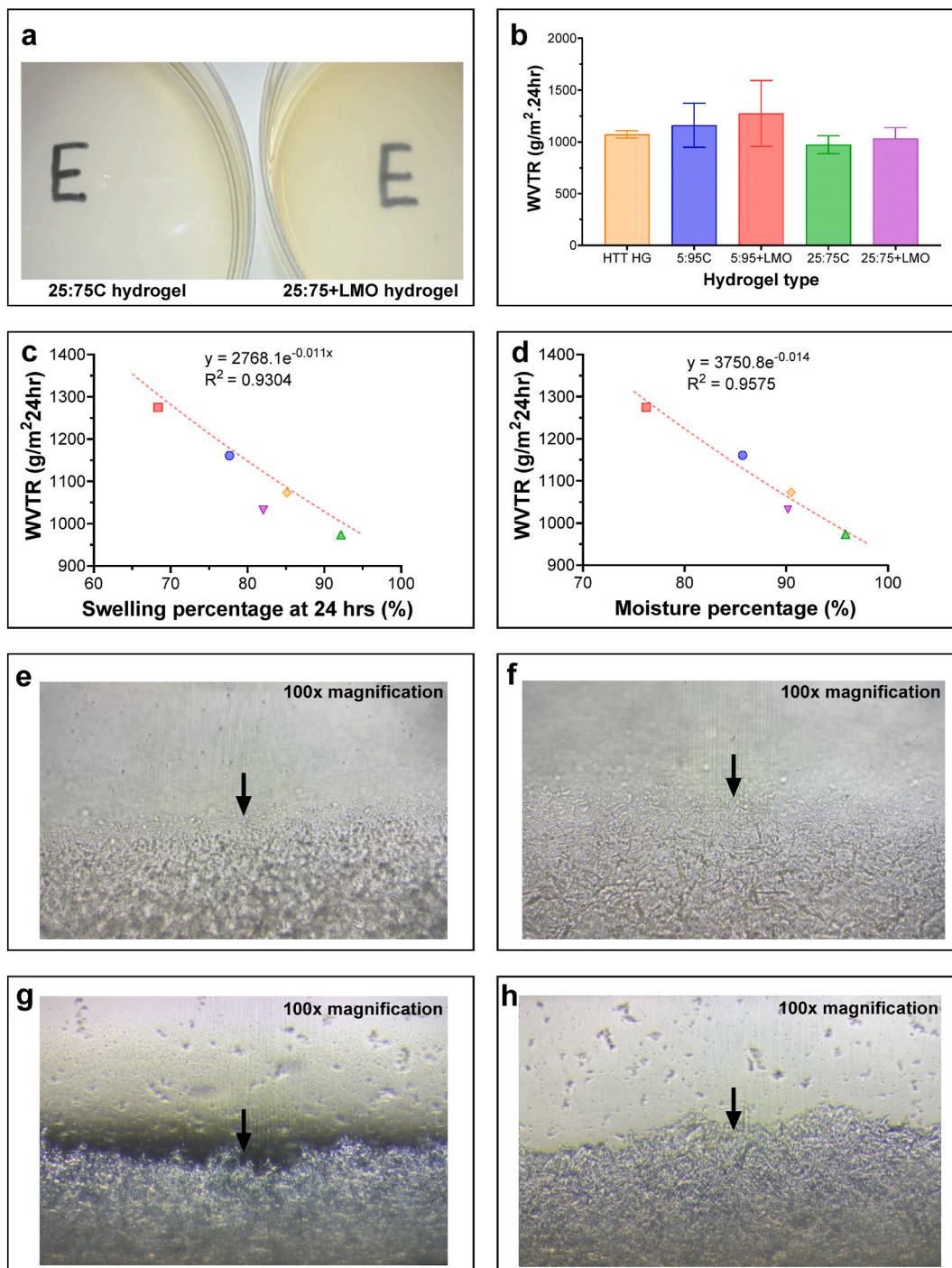

Fig. 5. Water vapour transmission rate (WVTR) analysis. a) Representative photos of 25:75C and 25:75+LMO hydrogel films (no magnification) illustrating the light transmission characteristic. b) The rate at which water vapour was transmitted through hydrogel films in 24 h. Data represented as mean ± SEM. The relationship of WVTR with c) swelling percentage at 24 h and d) moisture percentage. ----- represents the line of best fit for presented data sets. Legend: ◆ HTT HG, ● 5:95C, ■ 5:95+LMO, ▲ 25:75C and ▼ 25:75+LMO. Compound light microscope images of the interface between the hydrogel and culture plate (indicated by black arrows): e) and f) 25:75C hydrogels and g) and f) 25:75+LMO hydrogel films obtained using an Olympus CKX53 (100× magnification).

dominant. However, 25:75+LMO hydrogels compared to the 25:75C hydrogels displayed a decrease in G".

A G' > G″ was displayed in 5:95C, 5:95+LMO and 25:75+LMO hydrogels, whereas a G″>G′ was observed in 25:75C. The G′ dominance indicates primarily solid-like or elastic behaviour, which is representative of a viscoelastic hydrogel material. It is evident that as the swelling behaviour of these hydrogels increased, G' decreased (Fig. 4d) while both G" (Fig. 4e) and η* increased (Fig. 4f).

3.5. Water vapour transmission rate (WVTR) analysis

The transparency (light transmission), WVTR, and surface topography of the hydrogel prototypes along with its comparisons to swelling and moisture percentages are shown in Fig. 5.

Fig. 5a illustrates that the 25:75+LMO hydrogel was less transparent than the 25:75C hydrogel prototype. All hydrogels displayed very similar water vapour transmission properties with no significant differences reported between the commercial and experimental hydrogel prototypes. Although not statistically significant, Fig. 5b indicates that the WVTR is highest in the 5:95 hydrogels that include lemon myrtle oil, where the WVTRs of all the experimental hydrogel prototypes were similar to the commercial hydrogel. The WVTR of the 25:75+LMO hydrogels at 1032.34 ± 104.84 g/m^2 over 24 h was numerically the closest to the commercial dressing (1072.90 ± 34.53 g/m^2 over 24 h). Fig. 5c and d demonstrate that swelling and moisture retention capacities are inversely proportional to the WVTR, respectively. Fig. 5e–f illustrate the roughness of the hydrogels and the consistency within groups of each prototype. The incorporation of lemon myrtle oil improves the strength of the hydrogels as seen by the less diffuse interface between the hydrogels and the culture plate plastic (see arrows). This supports the data in Fig. 4a demonstrating the more solid-like behaviour of the 25:75+LMO compared to the 25:75C prototype.

3.6. Protein adsorption assay

The adsorption densities of the protein bovine serum albumin (BSA) into the hydrogel prototypes are displayed in Fig. 6a, and the relationship with hydrogel thicknesses displayed in Fig. 6b.

Fig. 6a displays reduced levels of protein adsorption onto hydrogels with higher sodium alginate levels (5:95C and 5:95+LMO). As the thickness of the hydrogel increases, an increased protein adsorption onto the hydrogel surfaces is displayed (Fig. 6b). Overall, the results suggest that the incorporation of lemon myrtle oil, higher levels of aloe vera and lower levels of sodium alginate can increase protein adsorption of the hydrogel. A protein adsorption of 0.352 ± 0.001 mg for 25:75+LMO hydrogels was similar to the commercial dressing (0.374 ± 0.001 mg), which could be due to the 25:75+LMO hydrogels having a similar hydrogel moisture percentage to the commercial dressing (Fig. 3b) allowing similar levels of protein adsorption.

3.7. Antimicrobial activity assay

The antimicrobial activity of the experimental and commercial hydrogels was tested via a two-stage process. Firstly, using a 96-well plate, broth microdilutions were analysed for microbial growth (Fig. 7a), followed by streaking analysis using Sensitest agar plates (Fig. 7b).

Fig. 7a illustrates that the 5:95C hydrogels support full growth of *S. epidermidis* and *C. albicans* the same as the controls, whereas
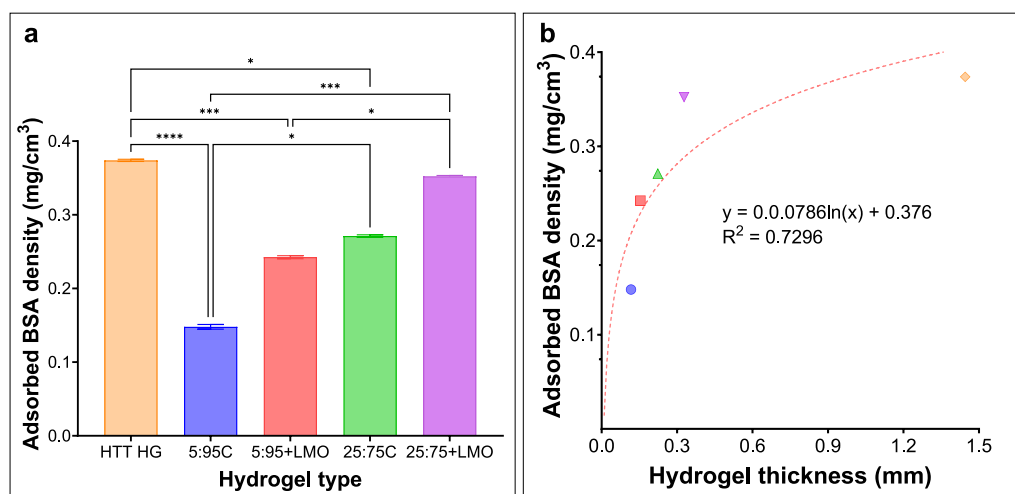

Fig. 6. Protein adsorption assay. a) The adsorbed BSA density by hydrogel prototypes after 24 h. Data represented as mean ± SEM. *$p \leq 0.05$, ***$p \leq 0.001$, ****$p \leq 0.0001$ and b) The relationship of adsorbed BSA density with thickness of hydrogel films. ----- represents the line of best fit for presented data sets. Legend: ◆ HTT HG, ● 5:95C, ■ 5:95+LMO, ▲ 25:75C and ▼ 25:75+LMO.
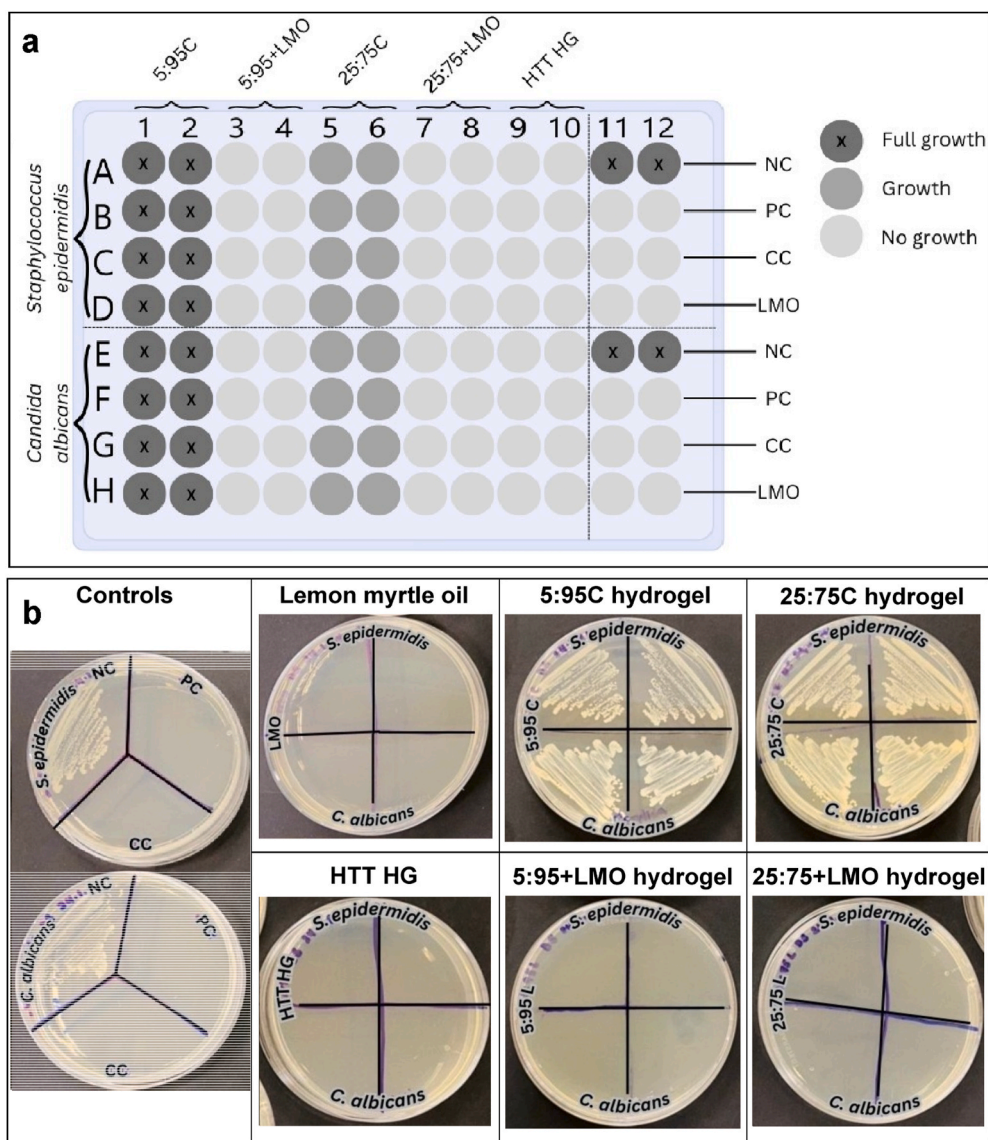
Fig. 7. Antimicrobial susceptibility broth microdilution test. *Staphylococcus epidermidis* and *Candida albicans* were tested via a) 96-well broth microdilution test and b) Sensitest agar plate streaking to determine the antimicrobial activity of lemon myrtle oil and the experimental and commercial hydrogels by comparing them to negative control (NC; sterile water), positive control (PC; ciprofloxacin for *S. epidermidis* and amphotericin B for *C. albicans*), contamination control (CC; Muller-Hinton Broth and RPMI media without microbes for *S. epidermidis* and *C. albicans*, respectively).

25:75C hydrogels demonstrated comparably less growth. These results are also supported by the streak tests shown in Fig. 7b. When lemon myrtle oil was evaluated by itself and incorporated into the hydrogels (5:95+LMO and 25:755+LMO), no microbial growth was displayed (Fig. 7a), which is further supported by the streak test in Fig. 7b. This verifies that lemon myrtle oil and 5 μg/mL LMO-containing hydrogels demonstrate antimicrobial activity against *S. epidermidis* and *C. albicans*. The hydrogels also maintain their structural integrity at room temperature for at least three months.

4. Discussion

The hydrogel prototype with an aloe vera: sodium alginate ratio of 25:75 supplemented with 5 μg/mL lemon myrtle oil displayed the most comparable physicochemical properties to the commercial hydrogel-based wound dressing. FTIR spectral analysis confirmed that the chemical structure and molecular interactions of the hydrogel matrices were similar to the commercial dressing. The 25:75C and 25:75+LMO prototypes were also biocompatible with the HaCaT human keratinocyte secondary cell line and also stimulated HaCaT cell proliferation over 24, 48, and 72 h of culture. The 25:75+LMO formulation also demonstrated moisture retention, water

absorption, protein adsorption, and antimicrobial activity closely mimicking the properties of the commercial dressing.

Published studies have used the human keratinocyte cell line HaCaT as a predictor of *in vivo* biocompatibility of developed hydrogel prototypes [27]. Improved cell migration, reduced cell apoptosis, and increased cell viability and proliferation have been reported as indicators of biocompatibility. Therefore, the current study used HaCaT cells to investigate the biocompatibility of the 25:75C and 25:75+LMO hydrogel prototypes. In the presence of 25:75+LMO hydrogels, there was a significantly increased level of cell viability compared to the control group (no hydrogel) and the 25:75C hydrogels. These results indicate that the 25:75C and 25:75+LMO hydrogel prototypes are biocompatible with human keratinocyte cells. Other *in vitro* studies have used dermal fibroblast cell lines (HDFs) as well as *in vivo* models including murine and porcine skin [28].

One of the major benefits of hydrogel-based wound dressings over traditional gauze-type dressings and a characteristic of the hydrogel prototypes produced in this study was swelling behaviour and moisture capacity (percentage). These physicochemical properties reflect the hydrogel film's *in vivo* potential to absorb excessive wound exudate and maintain the moisture balance within the wound microenvironment to promote wound healing [29]. The balance between moisture retention and release protects the wound against excessive dehydration or excessive accumulation of harmful exudates. A hydrogel wound dressing needs to also maintain a thickness that enables it to mimic healthy skin and the underlying extracellular matrix, thereby enabling the restoration of normal cell signalling pathways [30] and stimulating fibroblast cell proliferation leading to wound closure [31]. Although the AV:SAC and AV:SA + LMO hydrogel prototypes in this study were thinner than the commercial dressing, the 25:75+LMO had all other comparable physicochemical properties with the commercial dressing.

Previous research has demonstrated that increasing the percentage of sodium alginate in hydrogels increases ionic crosslinking density due to the increased interaction between calcium ions and the carboxylic groups of sodium alginate when hydrogels are crosslinked with $CaCl_2$ [6]. This results in the formation of a compact structure, which hinders the expansion of the polymer network due to limited penetration of fluid into the hydrogel matrix [32]. The resulting reduction in hydration of functional groups can lead to a reduction in swelling behaviour, moisture retention capability [33] and reduced hydrogel thickness. In this study, a lower ratio of sodium alginate compared to aloe vera was shown to have increased swelling behaviour and moisture retention and produce a thicker hydrogel. Further, the addition of lemon myrtle oil also produced a thicker hydrogel and increased swelling behaviour and moisture percentage. Previous research has demonstrated that lemon myrtle oil can promote crosslinking by increasing calcium ion diffusion, where lipid lumps are formed via coalescence and flocculation [34]. This can result in a poriferous structure, and the distribution of pores and cavities leading to accumulated free volume potentially increasing the hydrogel film thickness [35]. Other research into lemon myrtle oil has demonstrated that its hydrophobic properties can create the formation of a laminar structure that increases the gel fraction percentage by increasing hydrogel crosslinking rigidity [29]. The decreased WVTR with the increased ratio of aloe vera is also a favourable property to integrate into wound dressing hydrogels [36]. Furthermore, the immiscibility of lemon myrtle oil in water and weakened hydrogen bonds within the polymer matrix could allow the oil to leach out of the hydrogel films, resulting in an increased WVTR [37]. The WVTRs of the current study at 1000–1250 g/m^2 over 24 h are within the range of commercial hydrogel-based wound dressings [38].

The rheological analyses showed that the incorporation of higher aloe vera levels produces a more porous structure and enhanced miscibility in the hydrogel prototypes, where G' is lowered along with G'' and $\eta*$ as per the Cox-Merz rule that states the G'' tends to closely mirror the $\eta*$ trends at any given frequency [39]. The incorporation of lemon myrtle oil results in diminished crosslinking density and reduced fracture toughness due to weak polymer-oil interactions replacing strong polymer-polymer interactions [40]. Other studies have also reported that hydrogels with essential oil incorporation displayed a lower G' and $\eta*$ compared to hydrogels without essential oil [41]. The 5:95C, 5:95+LMO and 25:75+LMO hydrogels displayed $G'>G''$ indicating that elastic behaviour is dominant when a load is applied [42]. Conversely, $G''>G'$ in 25:75C, where the fluid-like property of the material is dominant where the material will behave as a viscoelastic mixture [43]. It should also be noted that as $\eta*$ decreases with increasing frequencies, all the hydrogel types will have pseudo-elastic properties with a shear-thinning behaviour [44]. The trends observed in 25:75+LMO hydrogels were similar to the trends reflected by the commercial dressing.

The protein adsorption behaviour of the hydrogel prototypes could also aid in wound healing and the protein adsorption capabilities of a wound dressing hydrogel are also an indicator of biocompatibility [45]. The adherence of serum proteins [45] and blood plasma proteins [46] onto the hydrogel surface supports the long-term performance of the hydrogel via enhancing biocompatibility with skin cells and the extracellular environment. Proteins act as ligands to bind to cell membrane receptors during adsorption, which promotes cell adhesion and cell proliferation [47]. The adherence of proteins in the form of a coating does not affect the mechanical stability of SA-based hydrogels [48], which can further be supported by the 25:75+LMO hydrogels having a similar BSA adsorption density to commercial HTT HGs.

Antimicrobial activity was demonstrated by the incorporation of lemon myrtle oil into the hydrogels. Interestingly, the 25:75 hydrogel prototype with a relatively higher ratio of aloe vera and lower sodium alginate imparted greater antimicrobial properties against *Staphylococcus epidermidis* and *Candida albicans* compared to the 5:95 prototype. When lemon myrtle oil was added, both prototypes exhibited complete inhibition of microbial growth. To our knowledge, this is the first study that has investigated the antimicrobial activity of lemon myrtle oil against *S. epidermidis* and *C. albicans* when incorporated in an AV-SA hydrogel film. Future experiments are required to test the antimicrobial activity of the hydrogel prototypes against a more diverse array of wound-associated microbes. The hydrogels with lemon myrtle oil incorporations (5:95+LMO and 25:75+LMO) displayed similar antimicrobial activity to the commercial dressing, where no microbial growth was observed. Therefore, it can be supported that increased aloe vera levels and the addition of lemon myrtle oil impart hydrogels with antimicrobial activity.

The cost of production for the most comparable hydrogel prototype with the commercial dressing, 25:75+LMO was estimated at AUD 50 per 100 g of hydrogel. As commercial wound dressings are priced at approximately AUD 85 per 100 g of hydrogel, further

investigation of this prototype is warranted. In addition to imparting anti-microbial properties and being biocompatible with human keratinocytes, the incorporation of lemon myrtle oil may also enhance the acceptance and use of hydrogel-based wound dressings made with lemon myrtle oil and other natural products in remote Australia as it incorporates First Nations knowledge.

5. Conclusions

This research successfully developed novel hydrogel prototypes produced with aloe vera, sodium alginate, and lemon myrtle oil for potential applications in wound dressings. The hydrogel prototype that was fabricated using aloe vera and sodium alginate in a ratio of 25:75 incorporating lemon myrtle oil, at a 5 μg/mL concentration, demonstrated comparable behaviour to a commercial hydrogel in physicochemical testing and demonstrated biocompatibility with the human keratinocyte HaCaT cell line and antimicrobial activity against the most common pathogenic wound microbes. These lower-cost hydrogel prototypes offer the potential to be used as cost-effective, sustainable hydrogel-based wound dressings. This study was limited to evaluating biocompatibility using an *in vitro* human skin cell line model; however, its findings support further investigation and optimisation using more complex in vit*r*o cell models and *in vivo* wound models.

Supporting information

Supporting Information is available from the Wiley Online Library or the author.

Data availability statement

The data that support the findings of this study are available from the corresponding author upon reasonable request.

CRediT authorship contribution statement

Dinuki M. Seneviratne: Writing – original draft, Visualization, Software, Methodology, Investigation, Formal analysis, Data curation, Writing – review & editing. **Brooke Raphael:** Writing – review & editing, Methodology, Investigation. **Eliza J. Whiteside:** Writing – review & editing, Visualization, Validation, Supervision, Software, Resources, Project administration, Methodology, Funding acquisition, Conceptualization, Data curation, Formal analysis, Investigation, Writing – original draft. **Louisa C.E. Windus:** Writing – review & editing, Supervision, Formal analysis, Conceptualization, Methodology, Software, Validation, Visualization, Writing – original draft. **Kate Kauter:** Writing – review & editing, Visualization, Validation, Supervision, Resources, Methodology, Formal analysis, Writing – original draft. **John D.W. Dearnaley:** Writing – review & editing, Methodology, Investigation, Writing – original draft. **Pratheep K. Annamalai:** Writing – review & editing, Visualization, Validation, Supervision, Methodology, Formal analysis, Conceptualization, Software, Writing – original draft. **Raelene Ward:** Writing – review & editing, Supervision, Conceptualization, Writing – original draft. **Pingan Song:** Writing – review & editing, Writing – original draft. **Paulomi (Polly) Burey:** Writing – review & editing, Visualization, Validation, Supervision, Resources, Project administration, Methodology, Funding acquisition, Formal analysis, Conceptualization, Investigation, Writing – original draft.

Declaration of competing interest

The authors declare that they have no known competing financial interests or personal relationships that could have appeared to influence the work reported in this paper.

References

[1] M. Berezo, J. Budman, D. Deutscher, C.T. Hess, K. Smith, D. Hayes, Predicting chronic wound healing time using machine learning, Adv. Wound Care 11 (6) (2022) 281–296, https://doi.org/10.1089/2Fwound.2021.0073.

[2] N. Graves, C.J. Phillips, K. Harding, A narrative review of the epidemiology and economics of chronic wounds, Br. J. Dermatol. 187 (2) (2022) 141–148, https://doi.org/10.1111/bjd.20692.

[3] M.J. Carter, J. DaVanzo, R. Haught, M. Nusgart, D. Cartwright, C.E. Fife, Chronic wound prevalence and the associated cost of treatment in Medicare beneficiaries: changes between 2014 and 2019, J. Med. Econ. 26 (1) (2023) 894–901, https://doi.org/10.1080/13696998.2023.2232256.

[4] P.E. Norman, D.E. Schoen, J.M. Gurr, M.L. Kolybaba, High rates of amputation among Indigenous people in Western Australia, Med. J. Aust. 192 (7) (2010), https://doi.org/10.5694/j.1326-5377.2010.tb03571.x, 421-421.

[5] D. Mijaljica, F. Spada, D.J. Klionsky, I.P. Harrison, Autophagy is the key to making chronic wounds acute in skin wound healing, Autophagy 19 (9) (2023) 2578–2584, https://doi.org/10.1080/15548627.2023.2194155.

[6] D. Thomas, M.S. Nath, N. Mathew, R. Reshmy, E. Philip, M.S. Latha, Alginate film modified with aloevera gel and cellulose nanocrystals for wound dressing application: preparation, characterization and in vitro evaluation, J. Drug Deliv. Sci. Technol. 59 (2020) 101894, https://doi.org/10.1016/j.jddst.2020.101894.

[7] F. Maunoury, A. Oury, S. Fortin, L. Thomassin, S. Bohbot, S. on behalf of the Explorer, Cost-effectiveness of TLC-NOSF dressings versus neutral dressings for the treatment of diabetic foot ulcers in France, PLoS One 16 (1) (2021) e0245652, https://doi.org/10.1371/journal.pone.0245652.

[8] W.S. Al-Arjan, M.U.A. Khan, H.H. Almutairi, S.M. Alharbi, S.I.A. Razak, pH-responsive PVA/BC-f-GO dressing materials for burn and chronic wound healing with curcumin release kinetics, Polymers 14 (10) (2022) 1949, https://doi.org/10.3390/polym14101949.

[9] K.K. Dey, S. Gayen, M. Ghosh, Structure and dynamics of sodium alginate as elucidated by chemical shift anisotropy and site-specific spin–lattice relaxation time measurements, Eur. Biophys. J. 50 (7) (2021) 963–977, https://doi.org/10.1007/s00249-021-01559-9.

[10] A. Khan, A. Andleeb, M. Azam, S. Tehseen, A. Mehmood, M. Yar, Aloe vera and ofloxacin incorporated chitosan hydrogels show antibacterial activity, stimulate angiogenesis and accelerate wound healing in full thickness rat model, J. Biomed. Mater. Res. B Appl. Biomater. 111 (2) (2023) 331–342, https://doi.org/10.1002/jbm.b.35153.

[11] İ. Kahramanoğlu, C. Chen, J. Chen, C. Wan, Chemical constituents, antimicrobial activity, and food preservative characteristics of aloe vera gel, Agronomy 9 (12) (2019) 831, https://doi.org/10.3390/agronomy9120831.

[12] I. Southwell, Backhousia citriodora F. Muell. (Lemon Myrtle), an unrivalled source of citral, Foods 10 (7) (2021) 1596, https://doi.org/10.3390/foods10071596.

[13] A.C. Lim, S.G.H. Tang, N.M. Zin, A.M. Maisarah, I.A. Ariffin, P.J. Ker, T.M.I. Mahlia, Chemical composition, antioxidant, antibacterial, and antibiofilm activities of Backhousia citriodora essential oil, Molecules 27 (15) (2022), https://doi.org/10.3390/molecules27154895.

[14] S.Y. Shim, J.H. Kim, K.H. Kho, M. Lee, Anti-inflammatory and anti-oxidative activities of lemon myrtle (Backhousia citriodora) leaf extract, Toxicol Rep 7 (2020) 277–281, https://doi.org/10.1016/j.toxrep.2020.01.018.

[15] P. Pereira, E.M. Mauricio, M.P. Duarte, K. Lima, A.S. Fernandes, G. Bernardo-Gil, M.-J. Cebola, Potential of supercritical fluid myrtle extracts as an active ingredient and co-preservative for cosmetic and topical pharmaceutical applications, Sustainable Chemistry and Pharmacy 28 (2022) 100739, https://doi.org/10.1016/j.scp.2022.100739.

[16] R. Pereira, A. Carvalho, D.C. Vaz, M.H. Gil, A. Mendes, P. Bártolo, Development of novel alginate based hydrogel films for wound healing applications, Int. J. Biol. Macromol. 52 (2013) 221–230, https://doi.org/10.1016/j.ijbiomac.2012.09.031.

[17] Y. Lu, Y. Wang, J. Zhang, X. Hu, Z. Yang, Y. Guo, Y. Wang, In-situ doping of a conductive hydrogel with low protein absorption and bacterial adhesion for electrical stimulation of chronic wounds, Acta Biomater. 89 (2019) 217–226, https://doi.org/10.1016/j.actbio.2019.03.018.

[18] Clinical and Laboratory Standards Institute, Performance Standards for Antimicrobial Susceptibility Testing; Eighteenth Informational Supplement, in CLSI Document M100-S18, Clinical and Laboratory Standards Institute, Pennsylvania, USA, 2008. ISBN 1-56238-653-0.

[19] C. Badita, D. Aranghel, C. Burducea, P. Mereuta, Characterization of sodium alginate based films, Rom. J. Phys. 65 (2020) 1–8.

[20] F. Dehghan, A. Gholipour-Kanani, M. Kamali Dolatabadi, S.H. Bahrami, Nanofibrous composite from polycaprolactone-polyethylene glycol-aloe vera as a promising scaffold for bone repairing, J. Appl. Polym. Sci. 139 (26) (2022) e52463, https://doi.org/10.1002/app.52463.

[21] A. Saarai, T. Sedlacek, V. Kasparkova, T. Kitano, P. Saha, On the characterization of sodium alginate/gelatine-based hydrogels for wound dressing, J. Appl. Polym. Sci. 126 (S1) (2012) E79–E88, https://doi.org/10.1002/app.36590.

[22] D. Bajer, K. Janczak, K. Bajer, Novel starch/chitosan/aloe vera composites as promising biopackaging materials, J. Polym. Environ. 28 (3) (2020) 1021–1039, https://doi.org/10.1007/s10924-020-01661-7.

[23] S. Beikzadeh, A. Akbarinejad, S. Swift, J. Perera, P.A. Kilmartin, J. Travas-Sejdic, Cellulose acetate electrospun nanofibers encapsulating Lemon Myrtle essential oil as active agent with potent and sustainable antimicrobial activity, React. Funct. Polym. 157 (2020) 104769, https://doi.org/10.1016/j.reactfunctpolym.2020.104769.

[24] M. Shafiq, M.T.Z. Butt, S.M. Khan, Synthesis of diethylene glycol-based aliphatic polyester polyol and effect of glycerin crosslinker on its properties, J. Polym. Res. 29 (9) (2022) 401, https://doi.org/10.1007/s10965-022-03199-9.

[25] A.R. Abbasi, M. Sohail, M.U. Minhas, T. Khaliq, M. Kousar, S. Khan, Z. Hussain, A. Munir, Bioinspired sodium alginate based thermosensitive hydrogel membranes for accelerated wound healing, Int. J. Biol. Macromol. 155 (2020) 751–765, https://doi.org/10.1016/j.ijbiomac.2020.03.248.

[26] S. Hasani, S.M. Ojagh, M. Ghorbani, Nanoencapsulation of lemon essential oil in Chitosan-Hicap system. Part 1: study on its physical and structural characteristics, Int. J. Biol. Macromol. 115 (2018) 143–151, https://doi.org/10.1016/j.ijbiomac.2018.04.038.

[27] Y. Liu, W. Xiong, C.-W. Wang, J.-P. Shi, Z.-Q. Shi, J.-D. Zhou, Resveratrol promotes skin wound healing by regulating the miR-212/CASP8 axis, Lab. Invest. 101 (10) (2021) 1363–1370, https://doi.org/10.1038/s41374-021-00621-6.

[28] H. Niu, Y. Guan, T. Zhong, L. Ma, M. Zayed, J. Guan, Thermosensitive and antioxidant wound dressings capable of adaptively regulating TGFβ pathways promote diabetic wound healing, Nature Partner Journals Regenerative Medicine 8 (1) (2023) 32, https://doi.org/10.1038/s41536-023-00313-3.

[29] F. Altaf, M.B.K. Niazi, Z. Jahan, T. Ahmad, M.A. Akram, A. safdar, M.S. Butt, T. Noor, F. Sher, Synthesis and characterization of PVA/starch hydrogel membranes incorporating essential oils aimed to be used in wound dressing applications, J. Polym. Environ. 29 (1) (2021) 156–174, https://doi.org/10.1007/s10924-020-01866-w.

[30] A. Chen, W. Huang, L. Wu, Y. An, T. Xuan, H. He, M. Ye, L. Qi, J. Wu, Bioactive ECM mimic hyaluronic acid dressing via sustained releasing of bFGF for enhancing skin wound healing, ACS Appl. Bio Mater. 3 (5) (2020) 3039–3048, https://doi.org/10.1021/acsabm.0c00096.

[31] J. Peng, H. Zhao, C. Tu, Z. Xu, L. Ye, L. Zhao, Z. Gu, D. Zhao, J. Zhang, Z. Feng, In situ hydrogel dressing loaded with heparin and basic fibroblast growth factor for accelerating wound healing in rat, Mater. Sci. Eng. C 116 (2020) 111169, https://doi.org/10.1016/j.msec.2020.111169.

[32] M. Kędzierska, M. Jamroży, S. Kudłacik-Kramarczyk, A. Drabczyk, M. Bańkosz, P. Potemski, B. Tyliszczak, Physicochemical evaluation of L-ascorbic acid and aloe vera-containing polymer materials designed as dressings for diabetic foot ulcers, Materials 15 (18) (2022) 6404, https://doi.org/10.3390/ma15186404.

[33] S. Sutthasupa, C. Padungkit, S. Suriyong, Colorimetric ammonia (NH3) sensor based on an alginate-methylcellulose blend hydrogel and the potential opportunity for the development of a minced pork spoilage indicator, Food Chem. 362 (2021) 130151, https://doi.org/10.1016/j.foodchem.2021.130151.

[34] M. Cofelice, F. Cuomo, A. Chiralt, Alginate films encapsulating lemongrass essential oil as affected by spray calcium application, Colloids and Interfaces 3 (3) (2019) 58, https://doi.org/10.3390/colloids3030058.

[35] J. Shin, S.-M. Seo, I.-K. Park, J. Hyun, Larvicidal composite alginate hydrogel combined with a Pickering emulsion of essential oil, Carbohydr. Polym. 254 (2021) 117381, https://doi.org/10.1016/j.carbpol.2020.117381.

[36] C.M.P. Yoshida, M.S. Pacheco, M.A. de Moraes, P.S. Lopes, P. Severino, E.B. Souto, C.F. da Silva, Effect of chitosan and aloe vera extract concentrations on the physicochemical properties of chitosan biofilms, Polymers 13 (8) (2021) 1187, https://doi.org/10.3390/polym13081187.

[37] H. Wang, Y. Liu, K. Cai, B. Zhang, S. Tang, W. Zhang, W. Liu, Antibacterial polysaccharide-based hydrogel dressing containing plant essential oil for burn wound healing, Burns & Trauma 9 (2021), https://doi.org/10.1093/burnst/tkab041.

[38] H.E. Salama, M.S. Abdel Aziz, Optimized alginate and aloe vera gel edible coating reinforced with nTiO2 for the shelf-life extension of tomatoes, Int. J. Biol. Macromol. 165 (2020) 2693–2701, https://doi.org/10.1016/j.ijbiomac.2020.10.108.

[39] C.V. Cervantes-Martínez, L. Medina-Torres, R.F. González-Laredo, F. Calderas, G. Sánchez-Olivares, E.E. Herrera-Valencia, J.A. Gallegos Infante, N.E. Rocha-Guzman, J. Rodríguez-Ramírez, Study of spray drying of the aloe vera mucilage (Aloe vera barbadensis Miller) as a function of its rheological properties, LWT - Food Sci. Technol. (Lebensmittel-Wissenschaft -Technol.) 55 (2) (2014) 426–435, https://doi.org/10.1016/j.lwt.2013.09.026.

[40] B.E. Alvarez-Perez, S. Bautista-Baños, G. Velazquez, M. Hernández-López, R.I. Ventura-Aguilar, C.A. Romero-Bastida, Application of chitosan bags added with cinnamon leaf essential oil as active packaging to inhibit the growth of Penicillium crustosum in D'Anjou pears, J. Polym. Environ. 31 (3) (2023) 1160–1172, https://doi.org/10.1007/s10924-022-02659-z.

[41] T.B. Goudoulas, S. Vanderhaeghen, N. Germann, Micro-dispersed essential oils loaded gelatin hydrogels with antibacterial activity, LWT (Lebensm.-Wiss. & Technol.) 154 (2022) 112797, https://doi.org/10.1016/j.lwt.2021.112797.

[42] B. Stubbe, A. Mignon, H. Declercq, P. Van Vlierberghe, P. Dubruel, Development of gelatin-alginate hydrogels for burn wound treatment, Macromol. Biosci. 19 (8) (2019) 1900123, https://doi.org/10.1002/mabi.201900123.

[43] A.A. Aldana, F. Valente, R. Dilley, B. Doyle, Development of 3D bioprinted GelMA-alginate hydrogels with tunable mechanical properties, Bioprinting 21 (2021) e00105, https://doi.org/10.1016/j.bprint.2020.e00105.

[44] F. Cuomo, M. Cofelice, F. Lopez, Rheological characterization of hydrogels from alginate-based nanodispersion, Polymers 11 (2) (2019) 259, https://doi.org/10.3390/polym11020259.

[45] A. Dodero, S. Scarfi, M. Pozzolini, S. Vicini, M. Alloisio, M. Castellano, Alginate-based electrospun membranes containing ZnO nanoparticles as potential wound healing patches: biological, mechanical, and physicochemical characterization, ACS Appl. Mater. Interfaces 12 (3) (2020) 3371–3381, https://doi.org/10.1021/acsami.9b17597.

[46] E. Saygili, E. Kaya, E. Ilhan-Ayisigi, P. Saglam-Metiner, E. Alarcin, A. Kazan, E. Girgic, Y.-W. Kim, K. Gunes, G.G. Eren-Ozcan, D. Akakin, J.-Y. Sun, O. Yesil-Celiktas, An alginate-poly(acrylamide) hydrogel with TGF-β3 loaded nanoparticles for cartilage repair: biodegradability, biocompatibility and protein adsorption, Int. J. Biol. Macromol. 172 (2021) 381–393, https://doi.org/10.1016/j.ijbiomac.2021.01.069.

[47] Y. Luo, Y. Li, X. Qin, Q. Wa, 3D printing of concentrated alginate/gelatin scaffolds with homogeneous nano apatite coating for bone tissue engineering, Mater. Des. 146 (2018) 12–19, https://doi.org/10.1016/j.matdes.2018.03.002.

[48] A. Schulz, M.M. Gepp, F. Stracke, H. von Briesen, J.C. Neubauer, H. Zimmermann, Tyramine-conjugated alginate hydrogels as a platform for bioactive scaffolds, J. Biomed. Mater. Res. 107 (1) (2019) 114–121, https://doi.org/10.1002/jbm.a.36538.